IOP Conf. Series: Materials Science and Engineering **1344** (2026) 012011 doi:10.1088/1757-899X/1344/1/012011

Performance simulation and model verification for a 20K thermal-coupled two-stage high-frequency pulse tube cryocooler

Bin Yang[1,2,3], Mingtao Pan[1,2,3], Bo Tian[1,2,3], Chenglong Liu[1,2,3], Jia Quan[1,2*], Yuexue Ma[1,2], Yanjie Liu[1,2], Houlei Chen[1,2], Miguang Zhao[1,2], Jingtao Liang[1,2,3]

[1] Technical Institute of Physics and Chemistry, Chinese Academy of Science, Beijing, China
[2] State Key Laboratory of Cryogenic Science and Technology, Technical Institute of Physics and Chemistry, Chinese Academy of Sciences, Beijing, China
[3] University of Chinese Academy of Sciences, Beijing, China

*E-mail: quanjia10@mail.ipc.ac.cn

Abstract. Currently, most high-precision infrared detectors used in space operate in the liquid hydrogen temperature range and require a two-stage pulse tube cryocooler (PTC) to provide a cryogenic environment. However, the existing two-stage thermal-coupled PTC suffer from low cooling capacity and efficiency. Therefore, in this study, the 2nd-stage of the PTC is considered as a whole system and a Sage model is established. The model is coupled with different inertance tube combinations to comprehensively simulate the performance. The simulation results are compared with the experimental results from the published article. The accuracy of the model simulation is verified. 70% of the simulated values for the no-load optimal frequency deviate from the experimental values by 0-1Hz. 84% of the simulated values for the cooling capacity at 20K deviate from the experimental values within a range of ±20%. It is observed that all experimental values for the optimal frequency at 20K is consistently 2-4Hz higher than the simulated values. The reasons are revealed from the perspective of the phase angle between the mass flow and pressure wave inside the 2nd-stage regenerator. The research results provide a foundation for the application of Sage software in the study of overall performance of two-stage thermal-coupled PTC.

1. Introduction

The absence of displacers and moving parts in pulse tube cryocoolers results in reduced vibration, longer lifespan and higher reliability[1], making them the preferred cryocooler option for space applications. In recent years, the development of space technology and deep space exploration has placed higher demands on the performance of cryocoolers operating at low temperatures. With an increasing number of high-precision detectors operating in the liquid hydrogen temperature range, there is a growing need for two-stage pulse tube cryocoolers to provide cooling in this temperature range. In 2020, Huang from Zhejiang University achieved 1.01W/20K cooling power using a cryocooler with an inertance tube reservoir for phase shifter and liquid nitrogen pre-cooling[2]. In 2021, Zhu from the Technical Institute of Physics and Chemistry, CAS, reported a two-stage thermal-coupled pulse tube cryocooler using inertance tube and reservoir for second-stage phase shifter, achieving 0.67W/20K cooling power[3]. In 2022, Jiang from the

Shanghai Institute of Technical Physics, CAS, presented an two-stage thermal-coupled pulse tube cryocooler using active phase shifter, achieving 1.15W/ 20K cooling power[4]. In 2023, Wang from the Shanghai Institute of Technical Physics, CAS, reported two-stage thermal-coupled pulse tube cryocooler using active phase shifter, achieving 1.87W/20K cooling power[5].

The phase shifter, as one of the key components affecting the performance of pulse tube cryocoolers, has undergone several innovations, including passive phase shifter such as small orifice and reservoir type, double-inlet type, inertance tube and reservoir type, as well as active phase shifter that introduce additional moving parts. Among these, the inertance tube and reservoir type is widely used in space applications due to its lack of moving parts, large phase shifting angles, and the ability to achieve more precise phase shifting through the combination of multiple stages of inertance tubes. However, conducting inertance tube shifting experiments is time-consuming and labor-intensive. Therefore, numerical simulations can be used to guide experimental investigations into the phase shifting capabilities of inertance tubes. Li conducted numerical simulations of the phase shifting capabilities of dual-segment inertance tubes used in pulse tube cryocoolers based on CFD software. They summarized a correction method for the CFD simulation results of the phase shifting capabilities of dual-segment inertance tubes[6]. Qu developed a one-dimensional model and combined it with response surface optimization to simulate the phase shifting performance of dual-segment inertance tubes. They discovered that the diameter of the second-segment inertance tube has a relatively small impact on the impedance magnitude at the inlet of the inertance tubes[7].

In a two-stage pulse tube cryocooler, the second-stage inertance tube operates in a cryogenic environment. Compared to single-stage pulse tube cryocoolers, conducting phase shifting experiments of the second-stage inertance tube in two-stage cryocoolers is more time-consuming and labor-intensive. Therefore, numerical simulation of the phase shifting capability of the second-stage inertance tube in two-stage pulse tube cryocoolers becomes more important. Hu utilized Sage software to simulate the second-stage of a two-stage pulse tube cryocooler and obtained the phase shifting characteristics of the second-stage inertance tube[8], providing guidance for experimental investigations. Currently, among various simulation software, Sage has shown good agreement between experimental and simulated results, and has become the primary software for pulse tube cryocooler calculations. Hence, in this study, Sage software was chosen to establish a model of the entire second-stage of pulse tube cryocooler, coupling different inertance tube combinations to simulate the cryocooler performance. The simulation results were compared with the experimental results from the published article "Experimental optimization of phase for a 20K thermally-coupled two-stage high-frequency pulse tube cryocooler"[9] to validate the accuracy and regularity of the model and provide guidance for experiments.

2. Cryocooler structure and Sage model

2.1 Cryocooler structure

Figure 1 shows a schematic diagram of the cryocooler structure. The lower box represents the first-stage cryocooler, which utilizes inertance tube and reservoir as the phase shifter. Its main function is to pre-cool the second-stage cryocooler through a thermal bridge. The upper box represents the second-stage cryocooler, which utilizes inertance tube, reservoir and double-inlet as the phase shifter. The letters in the Figure 1 respectively represent:

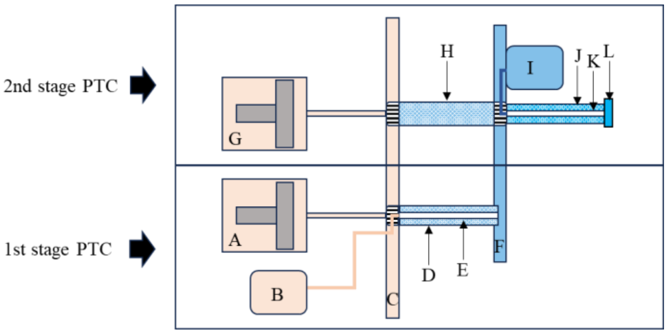

A. first-stage compressor; B. first-stage reservoir; C. hot-end flange; D. first-stage regenerator; E. first-stage pulse tube; F. thermal bridge; G. second-stage compressor; H. pre-regenerator; I. second-stage reservoir; J. second-stage regenerator; K. second-stage pulse tube; L. second-stage cold head.

Figure 1. Schematic diagram of pulse tube cryocooler structure

2.2 Sage Model

Sage is a computational software developed by Gedeon for Stirling cryocoolers. It is based on a first-order numerical method and allows for modeling and setting boundary conditions based on the actual cryocooler structure and experimental conditions. The principle involves discretizing and solving the continuity equation, momentum conservation equation and energy conservation equation for the cryocooler working fluid. After twenty years of development and iterative updates, Sage has achieved high accuracy. It can not only output the no-load cooling temperature and the cooling capacity at various temperatures, but also provide key parameters such as pressure waves, mass flow and phase angle of the intermediate components for analysis. Therefore, Sage software is chosen for numerical simulation.

In Sage, the flow is unidirectional, and two compressors cannot exist simultaneously. Therefore, the first-stage cryocooler is equivalent to a cold source with an experimental pre-cooling temperature of 80K. Additionally, the model is set up exactly according to the structure of the second-stage cryocooler as shown in Figure 1, with the pre-regenerator and second-stage regenerator filled with stainless steel wire mesh in layers according to the actual situation. To balance computational accuracy and speed, a time step of 9 is chosen. Furthermore, the parameters of the cryocooler and the boundary conditions of the model are listed in Table 1.

Based on the parameters and boundary conditions provided in the table 1, overall numerical model is established. To simultaneously monitor the no-load cooling temperature and the cooling capacity at 20K, the adiabatic boundary and isothermal boundary at 20K of the cold-end heat exchanger are set respectively to established two sets of corresponding numerical models. The schematic diagram of the latter model is shown in Figure 2.

Table 1. Dimensions of components and parameter settings in the Sage model

Component Name	Equivalent Diameter/mm	Length /mm	Material	Boundary Conditions
second-stage regenerator Ⅰ	21	22.5	titanium	adiabatic boundary
second-stage regenerator Ⅱ	21	22.5	titanium	adiabatic boundary
cold-end heat exchanger	21	2	copper	adiabatic boundary / isothermal boundary at 20K
pulse tube	10.2	60	titanium	adiabatic boundary

Based on the parameters and boundary conditions provided in the table 1, overall numerical model is established. To simultaneously monitor the no-load cooling temperature and the cooling capacity at 20K, the adiabatic boundary and isothermal boundary at 20K of the cold-end heat

exchanger are set respectively to established two sets of corresponding numerical models. The schematic diagram of the latter model is shown in Figure 2.

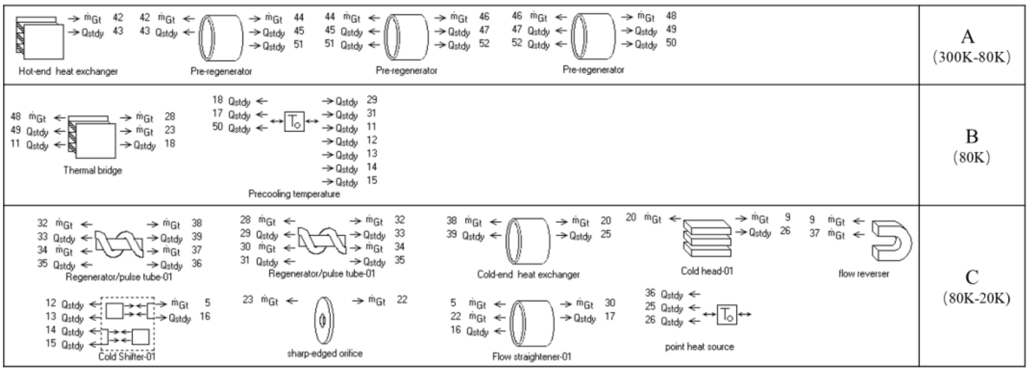

A: pre-regenerator; B: pre-cooling stage + thermal bridge; C: second-stag

Figure 2. Sage model of a 20K temperature range pulse tube cryocooler

3. Comparison of simulated and experimental results

According to the enthalpy flow phase-shifting theory, the phase angle between mass flow and pressure wave inside the cryocooler affects seriously the performance of the cryocooler. Typically, the performance of the cryocooler is improved by adjusting the length, diameter and combination of the inertance tube to match the impedance. Table 2 shows five sets of inertial tube combinations for phase optimization experiments from the published article “Experimental optimization of phase and compressor of a 20K thermal-coupled two-stage high-frequency pulse tube cryocooler”. Under identical conditions in terms of cryocooler dimensions, double-inlet orifice, pre-cooling temperature, regenerative material and filling ratio, the Sage model is utilized to simulate the key performance parameters, including no-load optimal frequency, no-load cooling temperature, optimal frequency at 20K and cooling capacity at 20K, for the five different combinations of inertance tubes at operating pressures ranging from 0.6 to 1.3 MPa. The simulated results will be compared with the experimental results cited in the reference.

Table 2. Inertance tube combination methods

Number	Type	Inertance Tube Combination Methods
case1	ternary-segment	Φ2mm×1.5m+Φ3mm×2m+Φ4mm×2m
case2	dual-segment	Φ3mm×2m+Φ4mm×2m
case3		Φ3mm×1m+Φ4mm×2m
case4		Φ3mm×1m+Φ4mm×3m
case5		Φ3mm×1.5m+Φ4mm×2m

3.1 Comparison of no-load optimal frequencies

Figure 3 compares the simulated and experimental values of the no-load optimal frequencies in different operation pressures for various inertance tube combinations in the cryocooler. In this context, the no-load optimal frequency is defined as the operating frequency at which the cryocooler achieves the lowest no-load cooling temperature. According to the simulation results, the order of the no-load optimal frequencies for the five inertance tube combinations is as follows: case3 > case4 ≈ case5 > case2 > case1. Additionally, when fixing a inertance tube combination, the no-load optimal frequency shows a slight increase with higher operation pressures, which is consistent with the experimental results. Over 70% of the simulated values differ from the experimental values by only 0-1 Hz, and these discrepancies may be attributed to differences between experiment and simulation , such as the joints with varying diameters and winding turns of the inertance tubes, as well as some parameter settings in the Sage model

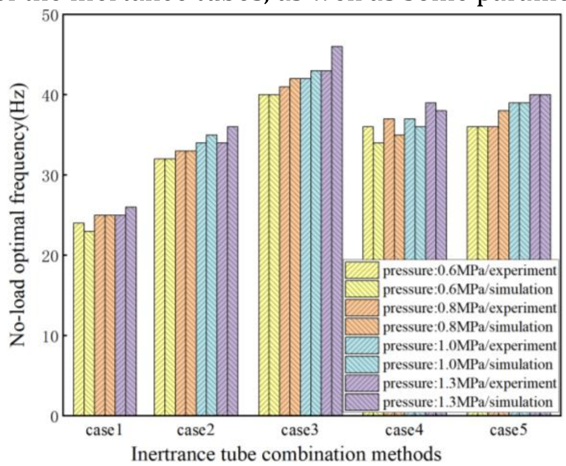

Figure 3. Comparison of no-load optimal frequencies

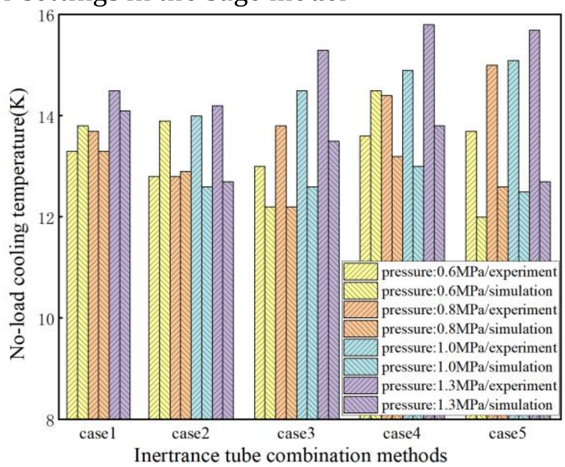

Figure 4. Comparison of no-load cooling temperatures

3.2 Comparison of no-load cooling temperatures

Based on the previous comparison of no-load optimal frequencies, it is known that there are slight differences between the simulated and experimental values. To facilitate the comparison of no-load cooling temperatures, the experimental values of the no-load optimal frequencies will be taken as the reference. The simulated and experimental values of the no-load cooling temperatures at this frequency will be compared in Figure 4.

According to the comparison results in Figure 4, the simulated values of the no-load cooling temperatures show a decreasing trend with increasing pressure at low pressures, different to the experimental values. But they increase with increasing pressure at high pressures, similar to the experimental values. This discrepancy is attributed to factors such as the filling of the regenerative material, joints with varying diameters and winding turns of the inertance tubes, which cause deviations in the impedance of the cryocooler from the model. Consequently, the experimental values of the optimal operation pressure are lower than the simulated values. Under the same operating conditions, approximately 80% of the simulated values are lower than the experimental values. This is due to the Sage model neglecting all radiative heat leakage and assuming adiabatic boundaries for components such as the second-stage regenerator and pulse tube, thereby disregarding radial heat leakage. Overall, there is a significant discrepancy between the simulated and experimental values of the no-load cooling temperatures, indicating a need for improvements in the model.

3.3 Comparison of optimal frequencies at 20K

It was also observed through simulations that, under the same inertance tube combination and operation pressure, the simulated values of the optimal frequency at 20K are consistently 2-4 Hz lower than the experimental values, as shown in Figure 5. To analyze the mechanism behind this phenomenon, let's take the case of coupling case5, operation pressure of 0.8 MPa, and PV power of 106 W as an example. Figure 6 shows the phase angle between the pressure waves and mass flow inside the second-stage regenerator within the frequency range of 30-40 Hz. According to the enthalpy flow phase-shifting theory, at the optimal frequency, the phase angle in the middle of the regenerator should be close to 0, and the phase angle at both ends should be symmetric. However, in the two-stage pulse tube cryocooler used in this study, the second-stage regenerator is filled in a layered manner, with half of the regenerator filled with a low mesh stainless steel wire mesh at the hot end and the other half filled with a high mesh stainless steel wire mesh at the cold end. This uneven filling leads to uneven pressure losses. Therefore, at the optimal frequency, the phase angle in the middle of the second-stage regenerator is not 0. Instead, the symmetry of the phase angle at both ends should be considered as the criterion for determining the optimal frequency at 20K. Based on the simulation results, it was found that at 36 Hz (the experimental value of the optimal frequency at 20K), the phase angle of the hot end was -35.5° and the phase angle of the cold end was 21.8°, indicating an asymmetric distribution. As the frequency decreases, the phase angle at both ends of the second-stage regenerator increases and gradually approaches symmetry. At 34 Hz (the simulated value of the optimal frequency at 20K), the phase angle of the hot end was -25.4° and the phase angle of the cold end was 26.8°, which is the closest to symmetry. This observation aligns completely with the simulated results of the optimal frequency at 20K. These deviations between the simulated and experimental values of the optimal frequency at 20K occur due to various factors that introduce deviations from the ideal model during the actual experimental processes such as manufacturing and assembly, resulting in a stable discrepancy between the simulated and experimental values.

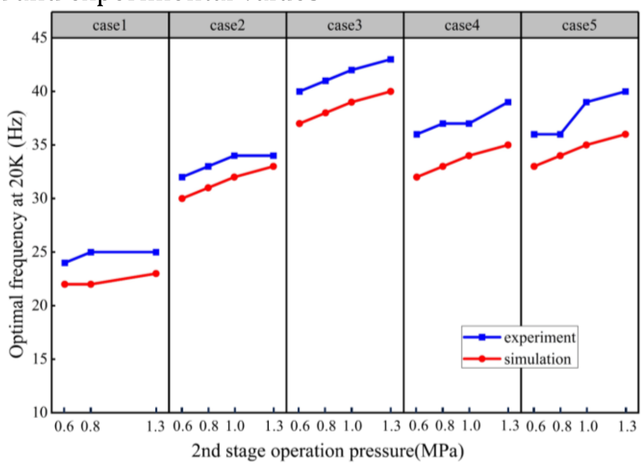

Figure 5. Comparison of simulated and experimental values for optimal frequencies at 20K

To further reveal the variation pattern of phase angles within the second-stage regenerator, simulations were conducted to analyze the phase variation of pressure waves and mass flow at the hot end, middle, and cold end of the regenerator. Figure 7 illustrates the variation of phase for pressure waves and mass flow at different locations within the regenerator with frequency. The phase of pressure waves exhibits significant changes with frequency, but when the frequency is fixed, the phase variation within the second-stage regenerator is relatively small with position. On the other hand, the phase of mass flow shows smaller variations with frequency, but when the frequency is fixed, the phase variation within the regenerator becomes more prominent with position. As the frequency increases, the phase of pressure waves at the hot end of the second-stage regenerator gradually decreases, while the phase of mass flow increases. Consequently, the phase angle between them decreases. Similarly, at the cold end of the second-stage regenerator, the phase of pressure waves also decreases gradually, while the phase of mass flow initially decreases and then increases. As a result, the phase angle between them decreases. At 34 Hz, the phase of pressure waves and mass flow at the hot end are 18.9° and 44.3°, respectively, resulting in a phase angle of -25.4°. At the cold end, the phase of pressure waves and mass flow are 18.6° and -8.2°, respectively, resulting in a phase angle of 26.8°. The phase angles at both ends of the two-stage regenerator are approximately symmetric, consistent with the previous simulation results.

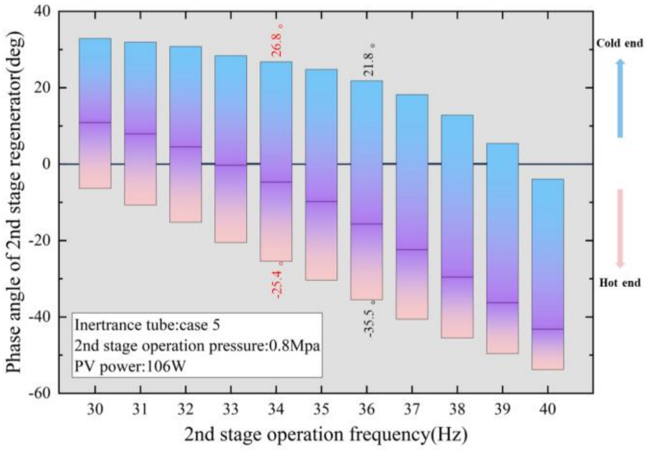

Figure 6. Variation of phase angle inside the second-stage regenerator with frequency

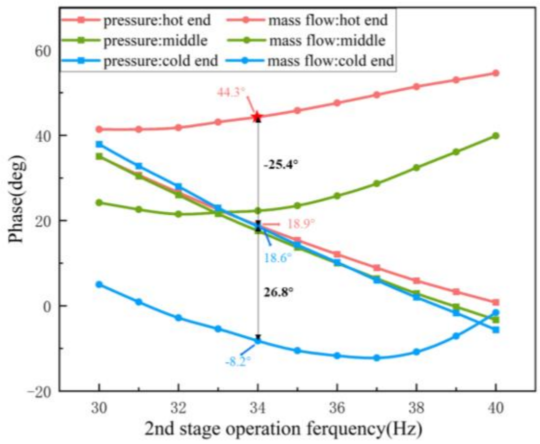

Figure 7. Variation of phase at the hot end, middle, cold end of the regenerator with frequency

3.4 Comparison of cooling capacity at 20K

According to the comparison results of the optimal frequency at 20K, the experimental values for the optimal frequency at 20K are 2-4Hz higher than the simulated values. To ensure the validity of the comparison of 20K cooling capacity, it is necessary to compare the cooling capacities of the cryocooler and the model at their respective optimal frequencies at 20K. Based on the comparison results in Figure 8, for the same operating conditions, the simulated values of the cooling capacity at 20K are lower than the experimental values for coupling cases 1-4, while the simulated value for coupling case 5 is higher than the experimental value. This discrepancy is due to the experimental value of the no-load cooling temperature for the cryocooler in coupling case 5 being much higher than the simulated value, resulting in the experimental value of the cooling capacity at 20K being smaller than the simulated value. Taking all measurement points into account, for the same operating conditions, over 84% of the simulated values deviate within ±20% compared to the experimental values.

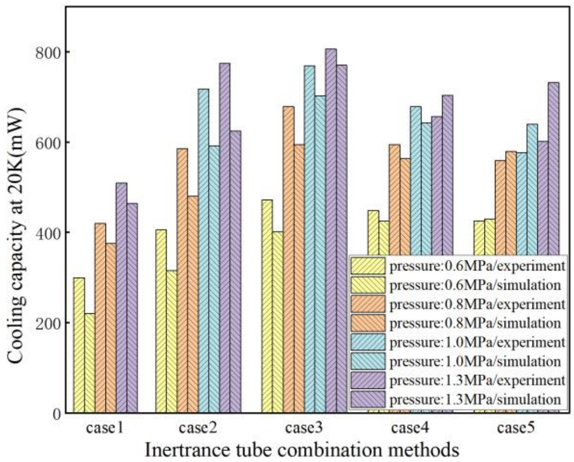

Figure 8. Comparison of cooling capacity at 20K

The wire mesh parameters set by the Sage model were measured using electron microscope, there may be measurement errors, leading to slight differences in regenerative capacity. Additionally, the experimental inertia tubes are wound in a spiral configuration, which differs from the straight-line arrangement used in the simulation, leading to slight differences in the phase shifting capability. Furthermore, since Sage is a one-dimensional model, it cannot account for three-dimensional heat transfer, which can also contribute to discrepancies between simulated and experimental values.

4. Conclusion

The first-stage of a two-stage thermal -coupled pulse tube cryocooler is equivalent to 80K heat source, and the second stage is regarded as the entire system to establish Sage model. To simultaneously monitor the no-load cooling temperature and the cooling capacity at 20K of the model, two sets of corresponding numerical models were established by setting different boundary conditions for the cold-end heat exchanger, including adiabatic boundary and isothermal boundary at 20K. The Sage model was coupled with five different inertia tube combinations to simulate the cryocooler performance. The simulation results were compared with the experimental results from the published article. This comparison validated the accuracy of the model in simulating the no-load optimal frequency and cooling capacity at 20K. Over 70% of the simulated values deviated from the experimental values by 0-1Hz for the no-load optimal frequency, and over 84% of the simulated values deviated within ±20% from the experimental values for the cooling capacity at 20K. However, the accuracy of the model in simulating the no-load cooling temperature is relatively low and requires further optimization. It is observed that all experimental values for the optimal frequency at 20K were consistently 2-4Hz higher than the simulated values. The reasons for this phenomenon were revealed from the perspective of the phase angle between the mass flow and pressure wave inside the second-stage regenerator, using the enthalpy flow phase-shifting theory.

Acknowledgments

This work is supported by National Key R&D Program of China under grant 2022YFB3903200, 2022YFB3903203.

References

[1] Chen GB, Tang K. The principle of a small cryogenic cryocooler (in Chinese) [M]. Beijing: Science Press, 2010.
[2] Huang C. Theoretical and experimental study on the pre-cooling method of Stirling pulse tube cryocooler in liquid hydrogen temperature rang (in Chinese) [D]; Zhejiang University, 2020.
[3] Zhu QL, Research on multi-stage high-efficiency pulse tube cryocooler in 20K temperature range (in Chinese) [D]; Technical Institute of Physics and Chemistry CAS, 2021.
[4] Zhenhua J, Jiantang S, Shaoshuai L, et al. Influence of frequency and pressure on entropy production characteristics of regenerator at 20 K pulse tube cryocooler[J]. International Journal of Refrigeration, 2022, 144: 222-230.
[5] Wang Y, Hui HJ, Wu WT, et al. A 910mW@15K thermal-coupled pulse tube cryocooler with active phase shifter [J]. Journal of Zhejiang University, 2023.
[6] Li SS, Chen X, Wei XB. Research on the simulation and correction method of phase shifting capacity of dual-segment inertance tube for pulse tube cryocooler (in Chinese) [J]. Journal of Dalian Minzu University, 2022, 24(5):424-428.
[7] Qu FJ, Yan CJ, Luo XK, et al. Study on phase shifting performance of dual-segment inertance tube of pulse tube cryocooler (in Chinese) [J]. Cryogenic engineering, 2023(5):1-7.
[8] Hu RZ, Zhu SW. Simulation and experimental studies of high-power pulse tube cryocooler in liquid hydrogen temperature range (in Chinese) [J]. Cryogenic engineering, 2023(5):24-28.
[9] Yang B, Gao m, Quan J, et al. Experimental optimization of phase for a 20K thermally-coupled two-stage high-frequency pulse tube cryocooler[C].29th International Cryogenic Engineering Conference 2024, IOP Conf. Series: Materials Science and Engineering 1327 (2025) 012056